Research Article

Evaluating adsorbent properties of drinking water treatment plant sludge-based carbons activated by K_2CO_3/CH_3COOH: a low-cost material for metal ion remediation

Carlos Magno Marques Cardoso[1] · Danilo Gualberto Zavarize[2] · Paulo de Assis Lago[1] · Marcelo Mendes Pedroza[3] · Sarah Silva Brum[1] · Andressa Regina Vasques Mendonça[1]

Abstract

Sludge reclaimed from drinking water treatment plant was carbonized and chemically activated by K_2CO_3 and CH_3COOH. The proposal was to evaluate its adsorbent properties as a low-cost alternative material for metal ion remediation. Morphological, physicochemical, and chemical characteristics have been presented and comprehensively discussed. Main findings revealed a surface area rich in mesopores and loaded with weakly acidic functional groups, also presenting an eroded aspect. Carbonization of the sludge's organic content increased the concentration of nitrogenic and oxygenated functional surface groups. Chemical activation by K_2CO_3 and CH_3COOH increased adsorption and desorption capacity, pore volume, and pore size by two, three, and over tenfolds, respectively. Uptake of cations increased by 51% and, for anions, around 27%. Association of carbonization with sequenced activation processes converted drinking water treatment plant sludge into an excellent and promising alternative adsorbent material.

Keywords Residue reclaiming · Chemical conversion · Alternative sources · Environment

1 Introduction

Severe levels of pollution have been compromising environmental quality around the world. Impacts on ecosystems and human health are leading to stringent laws that aim to control adverse effects caused by polluted environments. To maintain emission limits, the development of new technologies for treatment and disposal of industrial and non-industrial residues helps to comply with these environmental restrictions. Drinking water treatment plants (DWTPs), among all activities with the potential to cause environmental pollution, have a common problem regarding residue generation. The sludge formed during raw water treatment mostly comes from the coagulation, flocculation, and filtration steps. Its volume depends on operational conditions such as raw water quality, treatment technology, and the dosage of chemical coagulants [1].

The sludge from DWTPs is mainly composed of metal ions, settleable organic particles, and several types of microorganisms [2]. Due to these characteristics, the recycling in raw form has been tested for different purposes such as treatment of landfill leachate [3], adsorption processes [4–12], production of geopolymers [13], reuse as coagulant [14–17], application in agriculture [18], production of cement [19–21], sulfide control in sewers [22], production of ceramics [23, 24], and reuse in wastewater treatment [25, 26]. On the other hand, the utilization of this material in the form of activated carbon is rare. As far as we could find, a specific study by Rashed et al. [27] regarding the adsorption of methylene blue by drinking water treatment sludge after pyrolysis

and activation is available on the literature. Considering the lack of studies regarding the production of activated carbons from DWTP sludge, this study reports the conversion of this widely available feedstock through carbonization and chemical activation.

Activated carbons (AC) are scientifically known for having high sorption capacity for different types of chemical species [28], a characteristic of an adsorbent material with large surface area, porous structure, and chemically active surface [29]. Additionally, the high concentration of metals in raw water treatment sludge and, consequently, in its char, may also improve ion–solution interaction. Activated carbons usually have their surface functional groups bonded to complex aromatic rings, behaving similarly to aromatic hydrocarbons [30]. As so, a thermochemical modification would then improve these characteristics in the AC's surface chemistry, as a function of the usage purpose. Overall, the chemical activation of carbonized materials'

surface has been an alternative route to enhance either liquid or gaseous media adsorption processes.

To know better the potential of this material and spread its utility as a low-cost and worldwide available adsorbent for remediation processes, our study reports on the preparation of carbons with sludge from DWTP, chemically activated by K_2CO_3 and CH_3COOH, evaluating its adsorptive properties from a morphological, physicochemical, and chemical point of view.

2 Experimental procedures

Figure 1 shows a line diagram of the steps for the execution of this study. The procedures basically consisted of preparation of the crude sludge, production of the activated carbons and their characterization in terms of morphological, physicochemical, and chemical aspects.

Fig. 1 Line diagram of the steps for the execution of this study
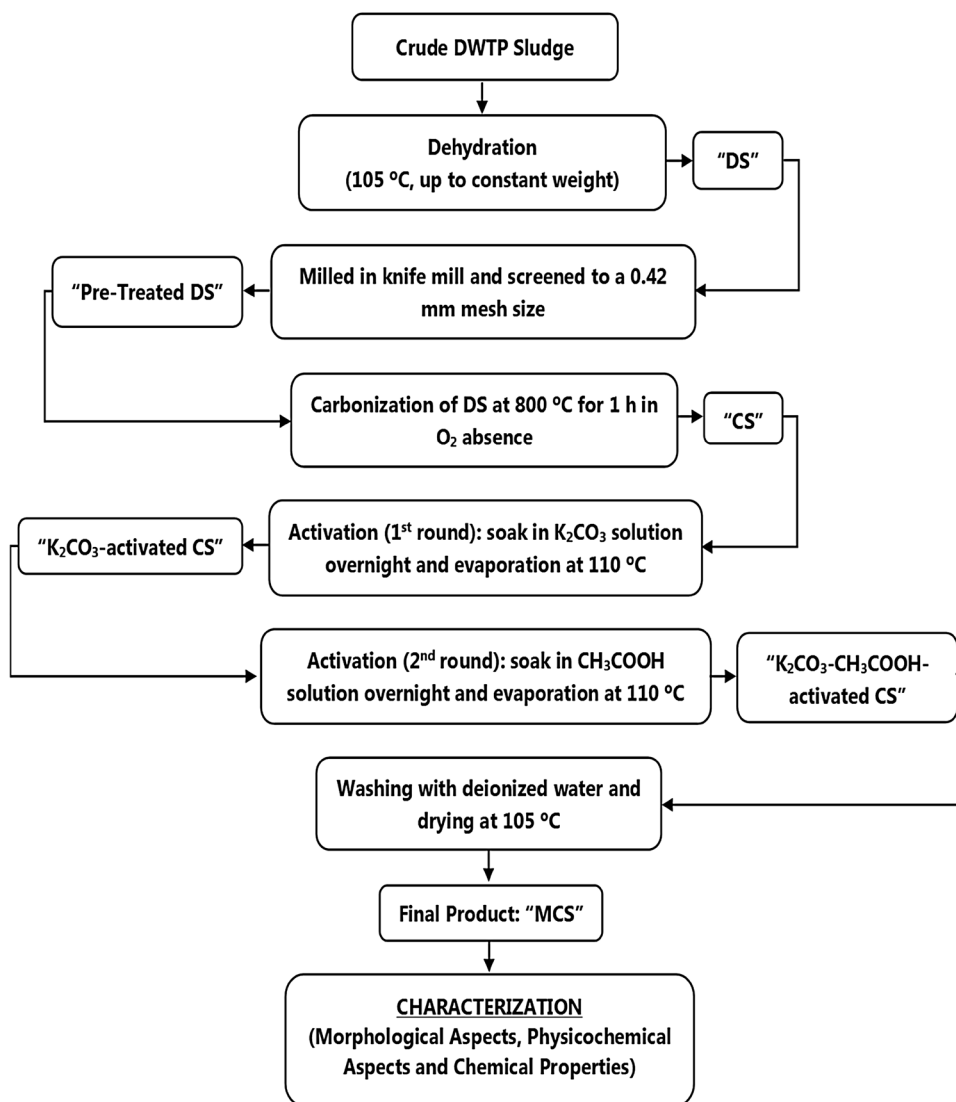
2.1 Material, reagents, and analytical methods

Drinking water treatment sludge (DWTS) was supplied by the Federal District's Sanitation Company (CAESB). Acetic acid, sodium bicarbonate, sodium carbonate, sodium hydroxide, sodium ethanolate, hydrochloric acid, sodium nitrate, and potassium carbonate were purchased from Synth (Labsynth®, Sao Paulo, Brazil). All analytical methods were conducted in a Varian Cary 5000 UV–Vis spectrophotometer. Cellulosic membranes (0.45 μm) were used for sample filtering. A Simpla PH-140 (ASKO, Sao Paulo, Brazil) was used to determine pH values.

2.2 Carbonization and activation of the sludge

A known amount of crude DWTP sludge was dehydrated in air-circulating oven SX 1.0 DTME (Sterilifer, Sao Paulo, Brazil) at 105 ºC up to constant weight and labeled "DS." Then, 100 g of DS was processed in a Thomas Model 4 knife mill (Wiley®, D. C., USA) and screened to a Mesh 40 size (Tyler Mesh Size 0.42 mm, W.S. Tyler, USA). Screened DS was carbonized in oxygen absence for 1 h using a muffle furnace (Thermo Scientific™ Thermolyne™ Industrial Benchtop) at 800 °C, and the resulting product was labeled as "CS." The first round of activation consisted of soaking overnight a known amount of CS in 100 mL of a 1 M solution of K_2CO_3, followed by evaporation at 110 °C. In the second round, K_2CO_3-impregnated CS soaked overnight in a 10:100 (m/v) solution of acetic acid (99.8% purity), also followed by evaporation at the same temperature. Final steps consisted of washing the activated carbons with deionized water up to neutral pH of the washing solution, then drying at 105 °C and labeling the final product as "MCS."

2.3 Characterization procedures

2.3.1 Morphology

Surface imaging of CS and MCS samples was captured in a JSM-7000F Field Emission Electron Scanning Microscope (JEOL, Tokyo, Japan) with accelerating voltage of 15 kV, after coating the samples with gold in a DII-29010SCTR Ion sputter. Surface area and distribution of pore size were determined by Barrett, Joyner, and Halenda (BHJ) method in a Quantachrome NOVA 1000 Series Analyzer (Anton Paar, New York, USA), absorbing and desorbing N_2 at 77.3 K for 2 h.

2.3.2 Physicochemical properties

Samples had pHpzc values estimated using the eleven-point method, described by Regalbuto and Robles [31].

The amount of acidic functional groups was determined by the Boehm method, as described by Kim and Park [32]. The capacity for cation and anion sorption was tested following the method described by Lu et al. [33].

2.3.3 Chemical properties

Contents of carbon, hydrogen, oxygen, nitrogen, and sulfur were obtained in a PerkinElmer 2400 Series II Elemental Analyzer. Metallic content (Al, As, B, Ba, Ca, Cd, Co, Cu, Fe, K, Mg, Mn, Mo, Ni, P, Pb, and Zn) was determined with an ICPE-9000 Multitype ICP Emission Spectrometer (Shimadzu®, Tokyo, Japan) following the methods of Hseu et al. [34]. Proximate analysis for moisture, volatile solids, ashes, and fixed carbon was carried out in a TGA7 Thermogravimetric Analyzer (PerkinElmer, Massachusetts, USA). Determination of organic matter composition (lignin, cellulose, hemicellulose, and extractives) followed the methods of van Soest and Robertson [35]. X-ray diffraction analysis was performed in a CubiX PRO Analytical X-ray Diffractometer (Phillips, Amsterdam, NL), equipped with a CuKα radiation source (40 kV, 55 mA, 1.5406 Å), nickel as filter media, 1 min^{-1} goniometer, 1 cm min^{-1} chart speed, and 2θ angles ranging from 5° to 80° in 0.2° steps. FTIR analysis occurred in a Cary 640 FTIR Spectrometer (Agilent Technologies, California, USA), mixing the samples with finely divided KBr at a 1:100 ratio, applying 4 cm^{-1} as spectral resolution and taking 16 scans per sample.

3 Results and discussion

3.1 Morphological aspects

Figure 2 shows the surface scanning of CS and MCS samples. The effects of carbonization and activation with K_2CO_3 gave to the material's surface an eroded aspect, and also widened and/or opened more pores. The protuberances seen on the MCS imaging refer to the presence of accumulated functional groups, provided by both the activation processes and the thermal degradation of organic matter, confirmed by the FTIR analysis. By comparing scans, CS presented a smoother, homogeneous, and micropores-rich surface with some random cracks, while MCS's surface showed heterogeneously distributed mesopores. BET analysis confirmed, posteriorly, these differences observed in the comparison. In the study of Rashed et al. [27], DWTP sludge was physically activated in a temperature range of 400 to 900 °C and chemically activated by acetic acid (0.1 to 3 M) and nitric acid (0.1 to 2 M), for the removal of methylene blue from aqueous solutions. They observed by analyzing SEM images that chemical activation by nitric acid had the greatest effect
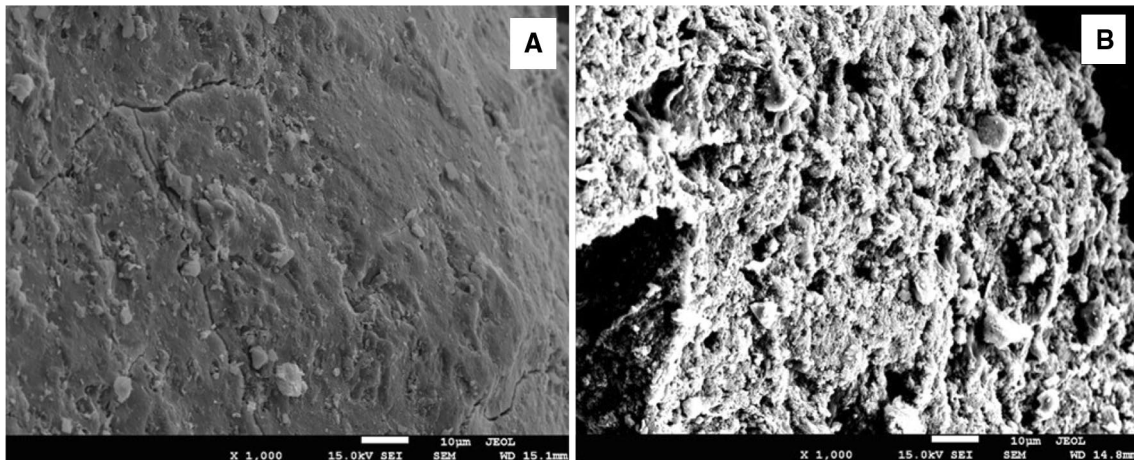
Fig. 2 SEM images of **a** carbonized sludge—CS, and **b** activated sludge char (MCS)

on the carbonized sludge compared to acetic acid. In terms of physical activation, the adsorbent surface was more impacted at a temperature of 500 °C.

Figure 3 shows the BET analysis of CS and MCS samples based on the BHJ method. Figure 3a depicts the adsorption and desorption of N_2 at 77.3 K. Despite similar form of the loops, the first round of activation increased MCS's absorbing and desorbing capacity in nearly twofolds (from 9.91 cm^3 g^{-1} to 18.04 cm^3 g^{-1}), also slightly enlarging the hysteresis between CS and MCS loops. BET surface area increased in nearly 21-folds (from 3.86 m^2 g^{-1} in CS to 79.86 m^2 g^{-1} in MCS). Figure 3b shows pore distribution increasing in approximately threefolds after the first round of activation (0.017 cm^3 g^{-1} in CS to 0.049 cm^3 g^{-1} in MCS). In CS, the composition of micro- and mesopores was 0.015 and 0.002 cm^3 g^{-1}, respectively, while in MCS, it changed to 0.016 and 0.033 cm^3 g^{-1}. Pore diameter was

nearly tenfolds higher (0.39 nm in CS to 3.77 nm in MCS), and, as seen in the graph, the interval from 0.3 to 4 nm holds the majority of pore diameters. Some studies postulated AC's adsorption and desorption capacity as not only dependent on the surface area, but also on the number of available binding sites and on their capacity of attracting molecules [36–38].

3.2 Analysis of chemical properties

Table 1 summarizes elemental, metallic, proximal, and organic composition analyses.

3.2.1 Elemental content

In terms of elemental content, data from Table 1 indicate that converting dried sludge into CS significantly
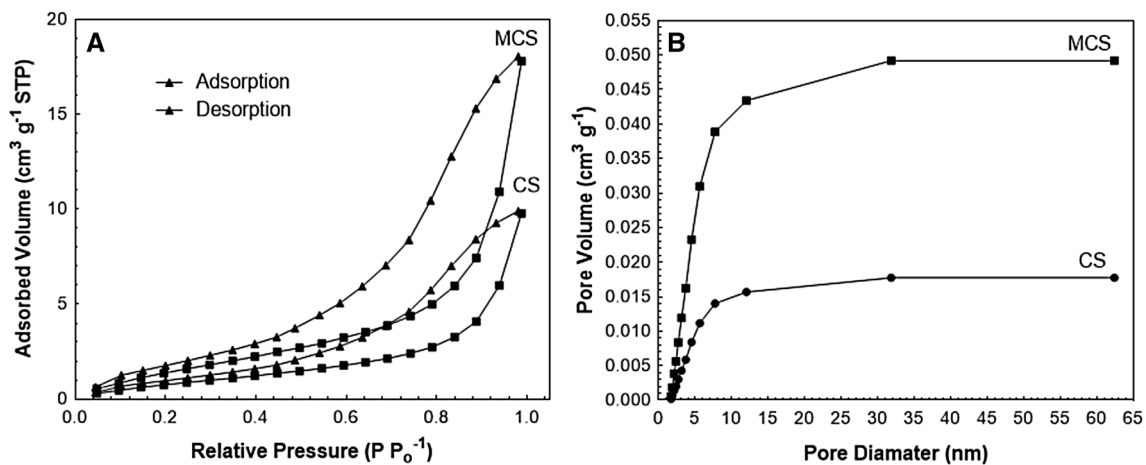
Fig. 3 N_2 adsorption–desorption isotherm (**a**) and pore size distribution (**b**) of CS and MCS

Table 1 Elemental, metal chemical, proximate, and organic composition of the samples

| Analyses		Samples		
		DS	CS	MCS
Elemental analysis (%)	C	66.42	72.74	76.97
	H	5.07	2.19	4.67
	O	22.51	11.25	15.41
	N	2.27	1.13	1.14
	S	3.73	1.79	1.81
Metal chemical analysis (mg L^{-1})	Al	108.0	87.73	85.47
	As	0.822	0.669	0.652
	B	0.045	0.037	0.036
	Ba	0.018	0.014	0.011
	Ca	0.894	0.727	0.709
	Cd	0.038	0.026	0.022
	Co	0.018	0.017	0.016
	Cu	0.019	0.018	0.017
	Fe	25.70	23.45	22.85
	K	3.93	2.350	9.289
	Mg	0.577	0.447	0.435
	Mn	0.924	0.853	0.832
	Mo	0.196	0.181	0.176
	Ni	0.026	0.024	0.020
	P	4.82	0.684	0.117
	Pb	0.058	0.055	0.054
	Zn	0.063	0.051	0.050
Proximate analysis (%)	Moisture	8.80	1.16	0.72
	Volatile solids	35.93	16.14	5.84
	Ashes	29.85	10.17	17.83
	Fixed carbon	25.42	72.53	75.61
Organic composition analysis (%)	Lignin	18.72	7.95	1.70
	Cellulose	2.87	1.43	0.69
	Hemicellulose	6.34	2.66	1.53
	Extractives	8.00	3.10	1.92

changed the amount of carbon, hydrogen, oxygen, nitrogen, and sulfur, but did not present expressive increases or decreases after the activation processes. Chen et al. [39] suggest that a typical activated carbon has 88% of C, 0.5% of H, 0.3% of N, 0.3 of S, and 9.9% of O. In CS, carbon content increased by 9%, while oxygen, hydrogen, nitrogen, and sulfur decreased by 50%, 57%, 51%, and 49%, respectively. In MCS, there was an increase of 14% in carbon content, while O, H, N, and S decreased by 32%, 8%, 50%, and 52%, respectively. Kacan [40] produced activated carbons with textile sewage sludge (TSSAC) by varying pyrolysis temperature (400 to 700 °C), pyrolysis time (45 to 150 min), and impregnation ratio (0.16 to 1.84) of the chemical agent of activation (KOH). The author observed that TSSAC with the highest BET area surface presented the lowest content of carbon and sulfur and the highest oxygen content.
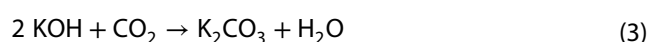
3.2.2 Metal chemical analysis

Analysis of metallic content shows decreases between 5 and 30% for almost all metals after the conversion into CS, except for K and P. The content of these two metals decreased by 40% and 86%, respectively. It may be attributed to the carbonization temperature above their ebullition points which is 758.8 °C for K and 280.5 °C for P [41, 42]. For MCS, the activation process led to decreases between 1 and 22% in metallic content. MCS's phosphorus content decreased by almost the same rate observed in CS, while the content of K increased by almost 75%, due to the chemical agent used in the first round of activation (K_2CO_3). In the study of Leng et al. [43], a biochar was produced from sewage sludge through liquefaction using acetone, ethanol, and methanol, at different temperatures (260 to 380 °C). The authors mention that metallic content increased in the biochars, compared to the sewage sludge, but their bioavailability and ecotoxicity were significantly relieved, which means safety of use. Similar observations were also made by Yuan et al. [44].

3.2.3 Proximate analysis

Proximate analysis data in Table 1 show moisture, volatile solids, and ash contents decreasing by nearly 87%, 56%, and 66% after conversion of DS into CS. The high content of ashes reflects a greater portion of inorganic matter in DS, which may be due to the presence of soil particles and other expanded minerals [27]. The content of fixed carbon increased by approximately 65% in CS, due to the presence of lignocellulosic matter, which favors adsorption capacity [39]. From CS to MCS, moisture and volatile solids kept decreasing (38% and 64%, respectively), while ash and fixed carbon were 76% and 5% higher. The type of carbonization and the organic and inorganic composition of the material generally reflect the results of proximate analyses [45]. In the case of our study, the increase in ashes and fixed carbon contents may be explained by two reasons. The first probable reason relates to the carbonization temperature [40]. The second reason may be due to double replacement reactions (DRR) occurring in the production of MCS [46]. On other words, water reacted with K_2CO_3 and formed 2 mols of KOH and 1 mol of CO_2, as shown in Eq. 1.

$$K_2CO_3 + H_2O \rightarrow 2KOH + CO_2 \tag{1}$$
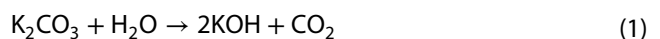
In Eq. 1, KOH is not equimolar to CO_2, and then, three possible events may occur: 1 mol of KOH reacts with CO_2 forming $KHCO_3$ (Eq. 2), or 2 mols of KOH reacts with CO_2 forming K_2CO_3 (Eq. 3), or the 1 mol of CO_2 from Eq. 1 reacts with 1 mol of H_2O forming H_2CO_3 (Eq. 4).

$$KOH + CO_2 \rightarrow KHCO_3 \tag{2}$$

$$2\,KOH + CO_2 \rightarrow K_2CO_3 + H_2O \tag{3}$$

$$CO_2 + H_2O \rightarrow H_2CO_3 \qquad (4)$$

If first there is formation of $KHCO_3$, as shown in Eq. 2, the residual mol of KOH seen in Eq. 1 will react with $KHCO_3$ forming K_2CO_3 and H_2O (Eq. 5). However, if it first forms H_2CO_3, as shown in Eq. 4, it will react with the residual mol of KOH and another one from the system to form K_2CO_3 and 2 mols of H_2O (Eq. 6). In any of these cases, the system equilibrates itself [46].

$$KHCO_3 + KOH \rightarrow K_2CO_3 + H_2O \qquad (5)$$

$$H_2CO_3 + 2\,KOH \rightarrow K_2CO_3 + 2H_2O \qquad (6)$$
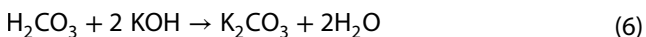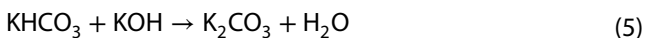
3.2.4 Organic composition analysis

Regarding organic composition analysis, lignin, cellulose, hemicellulose, and extractives contents decreased by approximately 58%, 51%, 59%, and 62% after the conversion of DS into CS. The activation processes also led to expressive decreases at the order of 79%, 52%, 43%, and 39%, respectively. In the case of CS, the high conversion temperature was the main reason. For MCS, the corrosive action of K_2CO_3 has probably been the cause for the continuous content decrease. Lignin is known for thermally decomposing over a wide temperature range (200–500 °C), forming products of low molecular weight, due of different oxygenated functional groups attached to its structure [47, 48]. These oxygenated functional groups start to cleave only in high temperatures, thus rearranging the polymeric backbone chain and resulting in 30 to 50 wt% of char production and releasing of gases [49]. The study of Jakab et al. [50] mentions that Na^+ and Ca^{2+} presence can strongly affect thermal decomposition of lignin by enhancing the charring reaction and formation of gases. About the content of extractives, Shebani et al. [51] and Poletto et al. [52] explain that their high volatility increases the material's ignitability even at lower temperatures, accelerating the degradation process. The content of hemicellulose, as seen in Table 1, was slightly higher than that of cellulose. Hemicellulose degradation occurs around 200 and 260 °C. It is less thermally stable than cellulose and generates more noncombustible gases and less tar [53]. About the content of cellulose, Balat [54] mentions that its thermal degradation follows the sequence: dehydration, hydrolysis, oxidation, decarboxylation, and transglycosylation, forming flammable gases. Then, at 450 °C, the production of volatile solids finishes and the cellulose starts to degrade as the temperature rises.

3.2.5 X-ray diffraction analysis

Figure 4 shows the XRD patterns for CS and MCS samples after the X-ray diffraction analysis.

They confirm the high presence of aluminum and iron ions. Some of the other metals previously analyzed by emission spectrometry were also visible in the XRD patterns. Similar peaks appear in other studies regarding raw water treatment sludge [55, 56]. The aluminum and iron high peaks relate to two main reasons: first, the treatment process for raw water and, second, the presence of settleable soil particles. As previously mentioned, sludge production occurs after applying considerable amounts of aluminum sulfate and ferric chloride in raw water, during the coagulation, flocculation, and filtration steps [1, 2]. In the case of the settleable soil particles, they usually come from the suction in the water body. Then, while executing the treatment, the chemicals, soil particles, and other impurities generate metal-rich biomass complexes (or floccules) which settle before going through filtration. In the case of our study, CAESB's sludge contains particles from latosol, rich in aluminic and ferric hydroxides [57].

Figure 5 illustrates the spectrums from FTIR analysis in CS and MCS samples. They show that CS and MCS have similar spectrums. However, MCS presented more prominent absorption bands.

Strong absorption peaks around 3400 and 3600 cm^{-1} correspond to -OH stretching, related to the increase in phenolic groups, described further in the surface functional groups analysis. Peaks around 2900 and 3000 cm^{-1} may represent vibrations of -COOH group [58], indicating that molecules of acetic acid from the second round of activation probably dissociated and bonded to MCS surface. Peaks from 1000 to 1200 cm^{-1} represent esters such as those present in ethers, phenols, and hydroxyl groups. The shoulder bonds observed in both CS's and MCS's spectrums probably are out-of-plane bending modes [59]. Formation of oxygenated surface groups and structures containing N–O bonds from the thermal degradation of organic matter relate to 1300 and 900 cm^{-1} peaks.

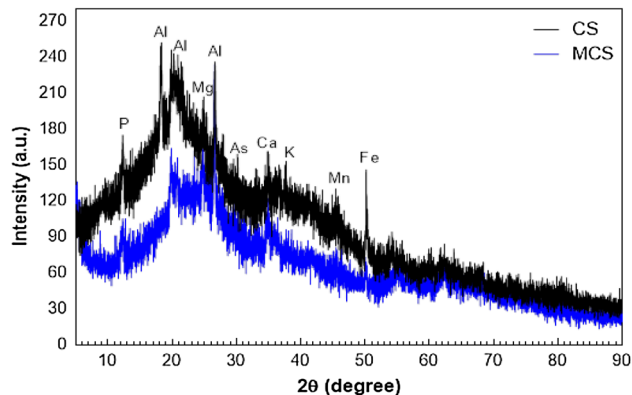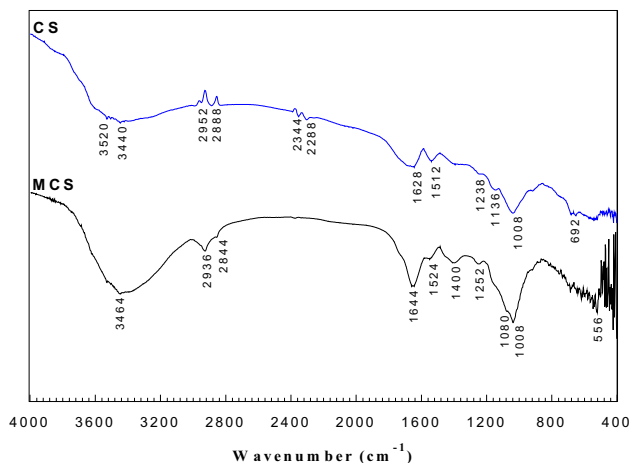**Fig. 4** X-ray diffraction patterns of CS and MCS

Fig. 5 FTIR spectrum of CS and MCS

El-Hendawy [60] suggests that they also relate to oxygen species of discrete nature.

3.3 Physicochemical aspects

3.3.1 Functional groups and pHpzc

Table 2 summarizes the type and concentration of weakly acidic functional groups found in DS, CS, and MCS surfaces, applying Boehm method. It also shows the concentration of basic functional groups and pHpzc values.

Changes in the concentration of functional groups from DS to CS were mainly due to the effect of carbonization. In the case of MCS, the main cause relates to the activation process. From Table 2, we infer that converting DS to CS influenced negatively on the concentration of all groups, presenting decreasing rates varying from 16% to 36%. On the other hand, the activation processes were beneficial for the carboxylic, phenolic, and carbonyl groups increasing their concentration in 37%, 56%, and 55%, respectively. Conversely, lactonic groups concentration decreased

Table 2 Surface chemical properties of the samples

Functional groups (mmol g^{-1})	Samples		
	DS	CS	MCS
Carboxylic groups	1.394	1.141	1.567
Lactonic groups	0.652	0.417	0.207
Phenolic groups	0.267	0.219	0.342
Carbonyl groups	1.211	1.019	1.581
Total acidity (mmol g^{-1})	3.524	2.796	3.697
Concentration of basic groups (mmol g^{-1})	0.49	0.63	0.54
pHpzc	5.30	6.80	5.05

by 51%. These benefits from the activation processes may relate to the presence of products from K_2CO_3 and CH_3COOH reactions, i.e., some oxidation reactions that converted carbonyl groups into carboxylic groups may have occurred.

Regarding pHpzc values, Regalbuto and Robles [31] explain that they represent the equilibrium net-surface charge of a given material. In other words, pHpzc values indicate equivalence between negative and positive charges. Figure 6 depicts the pHpzc values for DS, CS, and MCS. They show that converting DS into CS decreased total acidity considering that the pHpzc value increased by 35% (from 5.05 to 6.80). The activation processes returned MCS's acidic features, indicated by a pHpzc value of 5.30, 5% higher than DS and 22% lower than CS. These values evidenced the presence of weakly acidic functional groups, implying that acidic properties are more dominant after this type of activation.

3.3.2 Cation and anion uptake capacity

Figure 7 illustrates the uptake capacity for metal ions in DS, CS, and MCS. Absorption of cation (sodium) and anion (chlorine) was almost 83% and 43% higher in CS than in DS. From that, we inferred that carbonization had a positive effect on adsorbent capacity. Sodium and chlorine adsorption capacity in MCS samples was practically the same, differenced only by approximately 12%. If compared CS to MCS, the adsorption power for sodium and chlorine increased around 51% and 28%, respectively. By testing the sorption capacity of HNO_3-modified coconut fibers activated carbons, Lu et al. [33] reported increased Na^+ uptake as HNO_3 concentration in the activation process increased. In the case of our study, higher sorption capacities refer to several complexometric reactions occurring
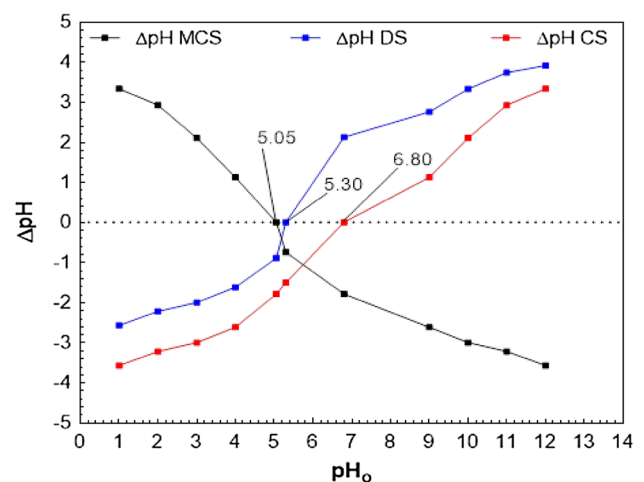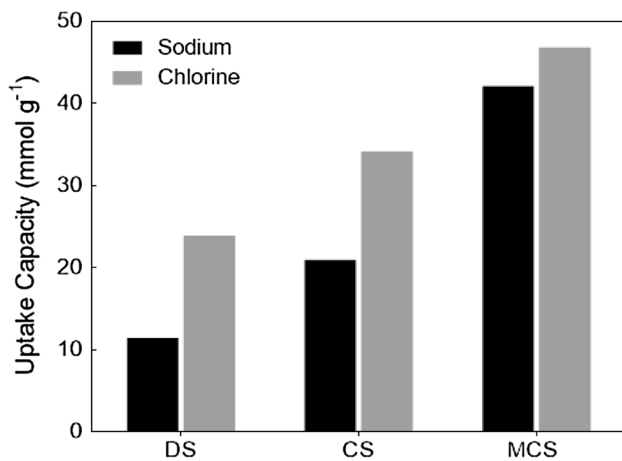

Fig. 6 Plot of the pHpzc values for DS, CS, and MCS

Fig. 7 Cation and anion capacity values for DS, CS, and MCS

after increasing carboxylic, carbonyl, and phenolic groups concentrations in MCS surface, as observed in the FTIR analysis.

4 Conclusions

Association of carbonization with sequenced activation processes converted DWTP sludge into an excellent and promising alternative adsorbent material. The facts that support this conclusion are: (1) the increased amount of mesopores which provided an eroded aspect to the surface and, consequently, more sites for chemical bonding, (2) higher surface area, pore volume, and pore size, and (3) increase in the concentration of weakly acidic functional groups which improved sorption capacity for cations and anions.

Compliance with ethical standards

Conflict of interest There are no any conflicts of interest regarding the content of this paper.

References

1. Ahmad T, Ahmad K, Alam M (2016) Characterization of water treatment plant's sludge and its safe disposal options. Procedia Environ Sci. https://doi.org/10.1016/j.proenv.2016.07.088
2. Bourgeois JC, Walsh ME, Gagnon GA (2004) Treatment of drinking water residuals: comparing sedimentation and dissolved air flotation performance with optimal cation ratios. Water Res. https://doi.org/10.1016/j.watres.2003.11.018
3. Hidalgo AM, Murcia MD, Gómez M, Gómez E, García-Izquierdo C, Solano C (2017) Possible uses for sludge from drinking water treatment plants. J Environ Eng. https://doi.org/10.1061/(ASCE)EE.1943-7870.0001176
4. Abo-El-Enein SA, Shebl A, Abo El-Dahab SA (2017) Drinking water treatment sludge as an efficient adsorbent for heavy metals removal. Appl Clay Sci. https://doi.org/10.1016/j.clay.2017.06.027
5. Nagar R, Sarkar D, Makris KC, Datta R (2010) Effect of solution chemistry on arsenic sorption by Fe- and Al-based drinking-water treatment residuals. Chemosphere. https://doi.org/10.1016/j.chemosphere.2009.11.034
6. Vinitnantharat S, Kositchaiyong S, Chiarakorn S (2010) Removal of fluoride in aqueous solution by adsorption on acid activated water treatment sludge. Appl Surf Sci. https://doi.org/10.1016/j.apsusc.2009.12.140
7. Zhou Y-F, Haynes RJ (2011) Removal of Pb(II), Cr(III) and Cr(VI) from aqueous solutions using alum-derived water treatment sludge. Water Air Soil Pollut. https://doi.org/10.1007/s11270-010-0505-y
8. Nawar N, Ahmad ME, El Said WM, Moalla SMN (2015) Adsorptive removal of phosphorous from wastewater using drinking water treatment-alum sludge (DWT-AS) as low-cost adsorbent. Am J Chem Appl 2(6):79–85
9. Jung K-W, Hwang M-J, Park D-S, Ahn K-H (2016) Comprehensive reuse of drinking water treatment residuals in coagulation and adsorption processes. J Environ Manage. https://doi.org/10.1016/j.jenvman.2016.06.041
10. Razali M, Zhao YQ, Bruen M (2007) Effectiveness of a drinking-water treatment sludge in removing different phosphorus species from aqueous solution. Sep Purif Technol. https://doi.org/10.1016/j.seppur.2006.12.004
11. Hovsepyan A, Bonzongo J-CJ (2009) Aluminum drinking water treatment residuals (Al-WTRs) as sorbent for mercury: implications for soil remediation. J Hazard Mater. https://doi.org/10.1016/j.jhazmat.2008.07.121
12. Dayton EA, Basta NT (2005) Use of drinking water treatment residuals as a potential best management practice to reduce phosphorus risk index scores. J Environ Qual. https://doi.org/10.2134/jeq2005.0083
13. Nimwinya E, Arjharn W, Horpibulsuk S, Phoo-ngernkham T, Poowancum A (2016) A sustainable calcined water treatment sludge and rice husk ash geopolymer. J Clean Prod. https://doi.org/10.1016/j.jclepro.2016.01.060
14. Ahmad T, Ahmad K, Ahad A, Alam M (2016) Characterization of water treatment sludge and its reuse as coagulant. J Environ Manage. https://doi.org/10.1016/j.jenvman.2016.08.010
15. Moghaddama SS, Moghaddama MRA, Arami M (2010) Coagulation/flocculation process for dye removal using sludge from water treatment plant: Optimization through response surface methodology. J Hazard Mater. https://doi.org/10.1016/j.jhazmat.2009.10.058
16. Nair AT, Ahammed MM (2013) The reuse of water treatment sludge as a coagulant for post-treatment of UASB reactor treating urban wastewater. J Clean Prod. https://doi.org/10.1016/j.jclepro.2013.12.037
17. Dayton EA, Basta NT (2001) Characterization of drinking water treatment residuals for use as a soil substitute. Water Environ Res. https://doi.org/10.2175/106143001X138688
18. Fan J, He Z, Ma LQ, Yang Y, Stoffella PJ (2014) Impacts of calcium water treatment residue on the soil-water-plant system in citrus production. Plant Soil. https://doi.org/10.1007/s11104-013-1881-z

19. Rodríguez NH, Martínez-Ramírez S, Blanco-Varela MT, Guillem M, Puig J, Larrotcha E, Flores J (2010) Re-use of drinking water treatment plant (DWTP) sludge: Characterization and technological behavior of cement mortars with atomized sludge additions. Cem Concr Res. https://doi.org/10.1016/j.cemconres.2009.11.012

20. Rodríguez NH, Martínez-Ramírez S, Blanco-Varela MT, Guillem M, Puig J, Larrotcha E, Flores J (2011) Evaluation of spray-dried sludge from drinking water treatment plants as a prime material for clinker manufacture. Cem Concr Comp. https://doi.org/10.1016/j.cemconcomp.2010.10.020

21. Alqam M, Jamrah A, Douglas H (2011) Utilization of cement incorporated with water treatment sludge. Jordan J Civ Eng 5:268–277

22. Sun J, Pikaar I, Sharma KR, Keller J, Yuan Z (2015) Feasibility of sulfide control in sewers by reuse of iron rich drinking water treatment sludge. Water Res. https://doi.org/10.1016/j.watres.2014.12.044

23. Kizinievič O, Žurauskienė R, Kizinievič V, Žurauskas R (2013) Utilisation of sludge waste from water treatment for ceramic products. Constr Build Mater. https://doi.org/10.1016/j.conbuildmat.2012.12.041

24. Benlalla A, Elmoussaouiti M, Dahhou M, Assafi M (2015) Utilization of water treatment plant sludge in structural ceramics bricks. Appl Clay Sci. https://doi.org/10.1016/j.clay.2015.09.012

25. Fragoso RA, Duarte EA (2012) Reuse of drinking water treatment sludge for olive oil mill wastewater treatment. Water Sci Technol. https://doi.org/10.2166/wst.2012.267

26. Babatunde AO, Zhao YQ, Doyle RJ, Rackard SM, Kumar JLG, Hu YS (2011) Performance evaluation and prediction for a pilot two-stage on-site constructed wetland system employing dewatered alum sludge as main substrate. Bioresour Technol. https://doi.org/10.1016/j.biortech.2011.02.065

27. Rashed MN, El-Daim El Taher MA, Fadlalla SMM (2016) Adsorption of methylene blue using modified adsorbents from drinking water treatment sludge. Water Sci Technol. https://doi.org/10.2166/wst.2016.377

28. Rufford TE, Zhu J, Hulicova-Jurcakova D (2014) Green carbon materials: advances and applications. CRC Press, USA

29. Çeçen F, Aktaş Ö (2011) Activated carbon for water and wastewater treatment: integration of adsorption and biological treatment. Wiley, Hoboken

30. Streat M, Malik DJ, Saha B (2004) Ion exchange and solvent extraction. Marcel Dekker, New York

31. Regalbuto JR, Robles JO (2004) The engineering of Pt/carbon catalyst preparation for application on proton exchange fuel cell membrane. University of Illinois at Chicago, Chicago. https://amrel.bioe.uic.edu/NSFREU2004/Reports2004/Jaime%20Robles_Final%20Report.pdf. Accessed 18 Nov 2018

32. Kim YS, Park CR (2016) Titration method for the identification of surface functional groups. In: Inagaki M, Kang F (eds) Materials science and engineering of carbon: characterization, 1st edn. Elsevier, Amsterdam, pp 273–286

33. Lu X, Jiang J, Sun K, Xie X, Hu Y (2012) Surface modification, characterization and adsorptive properties of a coconut activated carbon. Appl Surf Sci. https://doi.org/10.1016/j.apsusc.2012.05.029

34. Hseu Z-Y, Chen Z-S, Tsai C-C, Tsui C-C, Cheng S-F, Liu C-L, Lin H-T (2002) Digestion methods for total heavy metals in sediments and soils. Water Air Soil Pollut. https://doi.org/10.1023/A:1021302405128

35. van Soest PJ, Robertson JB (1980) Systems of analysis for evaluating fibrous feeds. In: Pidgen WJ, Balch CC, Graham M (eds) Standardization of analytical methodology for feeds. International Development Research Centre, Ottawa, pp 49–60

36. Nam S-W, Choi D-J, Kim S-K, Her N, Zoh K-D (2014) Adsorption characteristics of selected hydrophilic and hydrophobic micro-pollutants in water using activated carbon. J Hazard Mater. https://doi.org/10.1016/j.jhazmat.2014.01.037

37. Alabadi A, Razzaque S, Yang Y, Chen S, Tan B (2015) Highly porous activated carbon materials from carbonized biomass with high CO_2 capturing capacity. Chem Eng J. https://doi.org/10.1016/j.cej.2015.06.032

38. Perrich JR (2018) Activated carbon adsorption for wastewater treatment. CRC Press, Boca Raton

39. Chen X, Jeyaseelan S, Graham N (2002) Physical and chemical properties study of the activated carbon made from sewage sludge. Waste Manag. https://doi.org/10.1016/S0956-053X(02)00057-0

40. Kacan E (2016) Optimum BET surface areas for activated carbon produced from textile sewage sludges and its application as dye removal. J Environ Manage. https://doi.org/10.1016/j.jenvman.2015.09.044

41. Laksaci H, Khelifi A, Trari M, Addoun A (2017) Synthesis and characterization of microporous activated carbon from coffee grounds using potassium hydroxides. J Clean Prod. https://doi.org/10.1016/j.jclepro.2017.01.102

42. Ternero-Hildago JJ, Rosas JM, Palomo J, Valero-Romero MJ, Rodríguez-Mirasol J, Cordero T (2016) Functionalization of activated carbons by HNO_3 treatment: Influence of phosphorus surface groups. Carbon. https://doi.org/10.1016/j.carbon.2016.02.015

43. Leng L, Yuan X, Huang H, Shao J, Wang H, Chen X, Zeng G (2015) Bio-char derived from sewage sludge by liquefaction: characterization and application for dye adsorption. Appl Surf Sci. https://doi.org/10.1016/j.apsusc.2015.04.014

44. Yuan X, Huang H, Zeng G, Li H, Wang J, Zhou C, Zhu H, Pei X, Liu Z, Liu Z (2011) Total concentrations and chemical speciation of heavy metals in liquefaction residues of sewage sludge. Bioresour Technol. https://doi.org/10.1016/j.biortech.2010.12.055

45. García R, Pizarro C, Lavín AG, Bueno JL (2013) Biomass proximate analysis using thermogravimetry. Bioresour Technol. https://doi.org/10.1016/j.biortech.2013.03.197

46. Du M, Yu T, Wang F, Qu C (2019) Study on preparation of activated carbon from sludge. IOP Conf Ser Mater Sci Eng. https://doi.org/10.1088/1757-899X/484/1/012013

47. Brebu M, Vasile C (2010) Thermal degradation of lignin—a review. Cell Chem Technol 44:353–363

48. Goldstein IS (2018) Organic chemicals from biomass. CRC Press, Boca Raton

49. He Z (2017) Bio-based wood adhesives: preparation, characterization, and testing. CRC Press, Boca Raton

50. Jakab E, Faix O, Till F (1997) Thermal decomposition of milled wood lignins studied by thermogravimetry/mass spectrometry. J Anal Appl Pyrol. https://doi.org/10.1016/S0165-2370(97)00046-6

51. Shebani AN, van Reenen AJ, Meincken M (2008) The effect of wood extractives on the thermal stability of different wood species. Thermochim Acta. https://doi.org/10.1016/j.tca.2008.02.020

52. Polleto M, Zattera AJ, Santana RM (2012) Structural differences between wood species: evidence from chemical composition, FTIR spectroscopy, and thermogravimetric analysis. J Appl Polym Sci. https://doi.org/10.1002/app.36991

53. Speight JG (2011) The biofuels handbook. RSC Publishing, London

54. Balat M (2008) Mechanisms of thermochemical biomass conversion processes. Part 1: reactions of pyrolysis. Energy Source Part A. https://doi.org/10.1080/15567030600817258

55. Oliveira EMS, Machado SQ, Holanda JNF (2004) Caracterização de resíduo (lodo) proveniente de estação de tratamento de

águas visando sua utilização em cerâmica vermelha. Cerâmica. https://doi.org/10.1590/S0366-69132004000400007

56. Tartari R, Díaz-Mora N, Módenes N, Pianaro AS (2011) Generated sludge at water treatment station Tamanduá, Foz do Iguaçu, PR, as additive in red clay for ceramics: Part I: characterization of sludge and clay Paraná third plateau. Cerâmica. https://doi.org/10.1590/S0366-69132011000300006

57. Lopes AS, Guimarães Guilherme LR (2016) A career perspective on soil management in the Cerrado region of brazil. Adv Agron. https://doi.org/10.1016/bs.agron.2015.12.004

58. Silverstein RM, Bassler GC, Morrill TC (1981) Spectrometric identification of organic compounds. Wiley, New York

59. Puziy AM, Poddubnaya OL, Ritter JA, Ebner AD, Holland CE (2001) Elucidation of the ion binding mechanism in heterogeneous carbon-composite adsorbents. Carbon. https://doi.org/10.1016/S0008-6223(01)00048-3

60. El-Hendawy A-NA (2003) Influence of HNO_3 oxidation on the structure and adsorptive properties of corncob-based activated carbon. Carbon. https://doi.org/10.1016/S0008-6223(03)00029-0